Monatsh Chem (2010) 141:305–307
DOI 10.1007/s00706-010-0254-z

ORIGINAL PAPER

# Computational NQR study of a boron nitride nanocone

**Mahmoud Mirzaei · Azita Nouri · Masoud Giahi · Masoumeh Meskinfam**

Received: 16 October 2009 / Accepted: 15 January 2010 / Published online: 12 February 2010
© Springer-Verlag 2010

**Abstract** The electronic structure of a boron nitride nanocone with 240° disclination, and some properties that derive from this structure, were studied by density-functional theory calculations. In the considered model there are only hexagonal rings, with the apex and mouth of the nanocone saturated by hydrogen atoms. The model was optimized, and then the nuclear quadrupole resonance parameters were calculated at the sites of $^{11}$B and $^{14}$N nuclei. The results revealed that the nuclei in the boron nitride nanocone are divided into layers with similar electronic properties. The nuclei at the apex and mouth are very important for the electronic behavior of the nanocone, with $^{11}$B playing the major role.

**Keywords** Electronic structure · Electric field gradient · Nuclear quadrupole resonance · Density-functional theory

## Introduction

Following the discovery of carbon nanotubes (CNTs) [1], various forms of this fascinating novel material have been intensively studied employing a range of methods. Among these forms, nanocones have been observed either as caps at the end of nanotubes or as free-standing structures [2–4]. Further studies have also investigated the properties of nanocones, employing various theoretical and experimental techniques [5–7]. Since boron and nitrogen are neighbors of carbon in the Periodic Table, the combination of B and N yields the same number of electrons as two carbon atoms. Therefore, BN hetero-nanostructures are viewed as having similar, and in some cases better, properties compared with their C-based counterparts; for example, BN nanostructures are better semiconductors [8]. Boron nitride nanocones (BNNCs) have been characterized theoretically and synthesized [9–11]. When building such cones from a planar hexagonal sheet, various topological defects, e.g., pentagonal rings, occur at the apex. In BNNCs, this pentagonal ring defect causes at least one homonuclear B–B or N–N bond, yielding different electronic properties at the cone tip [12]; therefore, the study of possible terminations of BNNCs by appropriate techniques is an important subject.

The possibility of the formation of pentagonal rings including B–B and N–N homonuclear bonds at the apexes of BNNCs has been studied previously [5, 9]. However, to the best of the authors' knowledge, the possibility of a hexagonal ring at the apex of the nanocone, preventing the formation of homonuclear bonding, has not yet been studied. In this work, the electronic structure of a representative BNNC with 240° disclination and no pentagonal ring defect at the apex was studied by density-functional theory (DFT) calculations. To achieve this, the structure was optimized and the electric field gradient (EFG) tensors were calculated. EFG tensors at the sites of quadrupole nuclei, e.g., $^{11}$B and $^{14}$N, yield insights into the electronic and structural properties of the considered materials. Experimentally, nuclear quadrupole resonance (NQR) spectroscopy [13] measures the interaction energy between

M. Mirzaei (✉)
Department of Chemistry, Islamic Azad University, Shahr-e-Rey Branch, Shahr-e-Rey, Iran
e-mail: mdmirzaei@yahoo.com

A. Nouri
Department of Chemistry, Islamic Azad University, Shahr-e-Qods Branch, Shahr-e-Qods, Iran

M. Giahi · M. Meskinfam
Department of Chemistry, Islamic Azad University, Lahijan Branch, Lahijan, Iran

the EFG tensors and the nuclear electric quadrupole moment ($eQ$) as the quadrupole coupling constant ($C_Q$). Another important parameter is the asymmetry parameter ($\eta_Q$), which defines the deviation of the EFG tensor from cylindrical symmetry at the sites of quadrupole nuclei. Since the advantages of the calculation of NQR parameters for studying the electronic structure of BN nanostructures have been shown by recent studies [14, 15], we used this procedure to study the electronic structure of BNNCs.

## Results and discussion

Figure 1 shows two-dimensional (2D) views of the considered model, one rotated by 180°, indicating that the apex and mouth of the BNNC are terminated by heteronuclear atoms. In Fig. 1a, the apex is terminated by B and the mouth is terminated by N atoms, whereas in Fig. 1b the apex is terminated by N and the mouth is terminated by B atoms. The apex of the BNNC is not capped but is rather saturated by two hydrogen atoms, preventing the formation of pentagonal rings including homonuclear B–B and N–N bonds. The calculated bandgap energy of the considered BNNC is 3.51 eV, in agreement with the expected large bandgap of BN structures (~5.5 eV). The B–N bond lengths at the apex and mouth of the BNNC are 1.50 and 1.45 Å, respectively, and 1.46 Å at the other positions. The calculated NQR parameters are divided into 12 layers, with similar parameters in each layer (Table 1 and Fig. 1). This similarity indicates that the nuclei in each layer show similar electrostatic properties, resulting in similar NQR parameters.

In layer 1, the $C_Q$ values of $^{11}$B and $^{14}$N nuclei are 4.35 and 2.63 MHz, which are the largest values among the layers for each nucleus type. $C_Q$ depends on the orientation of the EFG tensor eigenvalues with respect to the $z$-axis ($q_{zz}$), which makes the major contribution to interactions with external agents. This means that the nuclei at the apex are very important for the electronic behavior of the BNNC. Furthermore, the larger $C_Q$ value of $^{11}$B compared with that of $^{14}$N indicates the major electronic role played by $^{11}$B at the apex of the BNNC. After layer 1, the largest magnitudes of the $C_Q$ values of $^{11}$B and $^{14}$N belong to layer 12, which forms the mouth of the BNNC. It is noted that terminating atoms at both the apex and the mouth are saturated by hydrogen atoms. In this layer, there are five $^{11}$B and five $^{14}$N nuclei, with similar NQR parameters (average values are reported in Table 1). The $C_Q$ values of

**Table 1** NQR parameters

| $^{11}$B | | | $^{14}$N | | |
|---|---|---|---|---|---|
| Layer | $C_Q$ (MHz) | $\eta_Q$ | Layer | $C_Q$ (MHz) | $\eta_Q$ |
| B1 | 4.35 | 0.24 | N1 | 2.63 | 0.79 |
| B2 | 2.76 | 0.20 | N2 | 1.43 | 0.45 |
| B3 | 2.82 | 0.11 | N3 | 1.64 | 0.42 |
| B4 | 2.63 | 0.15 | N4 | 1.00 | 0.50 |
| B5 | 2.73 | 0.07 | N5 | 1.00 | 0.31 |
| B6 | 2.64 | 0.09 | N6 | 0.74 | 0.38 |
| B7 | 2.69 | 0.04 | N7 | 0.72 | 0.30 |
| B8 | 2.65 | 0.05 | N8 | 0.59 | 0.28 |
| B9 | 2.64 | 0.02 | N9 | 0.58 | 0.38 |
| B10 | 2.65 | 0.05 | N10 | 0.58 | 0.46 |
| B11 | 2.66 | 0.09 | N11 | 0.85 | 0.75 |
| B12 | 3.32 | 0.24 | N12 | 2.16 | 0.88 |

See Fig. 1 for layer numbering

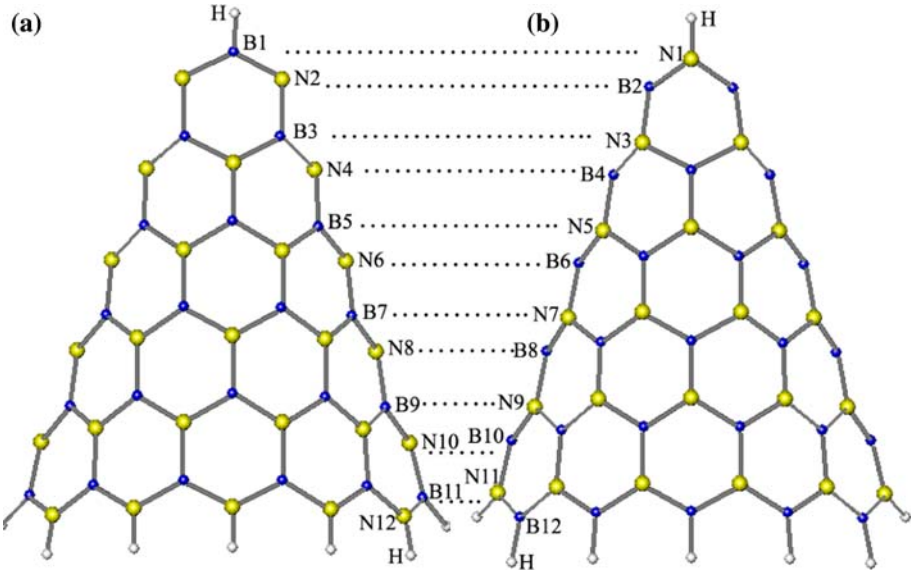


**Fig. 1** Front- and back-side (rotated by 180°) views of the cone model. *Dotted lines* indicate bonding between the two halves; the layers are numbered appropriately

$^{11}$B and $^{14}$N are 3.32 and 2.16 MHz; the value of $^{11}$B is still larger than that of $^{14}$N at the mouth of the BNNC, indicating the majority role played by $^{11}$B in the electronic behavior of the BNNC.

Boron and nitrogen have different electron valence shells, with a lone pair of electrons in the valence shell of nitrogen and no electrons in that of boron. Due to this different character of the valence shells, different electronic behavior is expected at the sites of these nuclei. Table 1 shows that the changes of the values of the obtained NQR parameters for layers 1 and 12 are notable, whereas those for the other layers of $^{11}$B nuclei are almost negligible. However, the most notable changes of the values of NQR parameters are observed for the layers of $^{14}$N nuclei. However, it is noted that the magnitude of the values for both nuclei reduces from the apex to the mouth of the BNNC, then increase immediately before the mouth.

## Conclusions

We studied the electronic structure of a BNNC with 240° disclination, and some properties that derive from this structure. The major difference between the considered model and those previously studied is that the present model has no pentagonal ring defect. The calculated NQR parameters at the sites of $^{11}$B and $^{14}$N nuclei reveal that the nuclei are divided into layers with similar electronic properties. The nuclei at the apex of the BNNC have the largest magnitudes of $C_Q$, with that for $^{11}$B being larger than that for $^{14}$N. The nuclei at the mouth of the BNNC also have large magnitudes of $C_Q$, although smaller than those at the apex. The large $C_Q$ values indicate the importance of the role played by the nuclei at the apex and mouth of the BNNC in its electronic behavior, with $^{11}$B being the most important.

## Computational details

As a representative model of a BNNC with 240° disclination, $B_{46}N_{46}H_{16}$ (Fig. 1) was considered in this study. Such nanocones commonly have pentagonal rings at the apex as a defect, resulting in homonuclear B–B and N–N bonds. However, there are just hexagonal rings in the considered model, with both the apex and mouth of the nanocone saturated by 2 and 14 hydrogen atoms, respectively. All-atom geometries of this structure were allowed to relax by performing optimization at the DFT level of theory, employing the BLYP method and 6-31G* standard basis set. Afterwards, EFG tensors at the sites of $^{11}$B and $^{14}$N nuclei were calculated in the optimized structure at the same theoretical level. Quantum-chemical calculations yielded the EFG tensors in the principal axes system (PAS) in the order: $|q_{zz}| > |q_{yy}| > |q_{xx}|$; therefore, directly relating to the experiments, Eqs. (1) and (2) were used to generate the NQR parameters ($C_Q$ and $\eta_Q$). The standard $Q$ values reported by Pyykkö [16] are employed in Eq. (1): $Q(^{11}\mathrm{B}) = 40.59$ mb and $Q(^{14}\mathrm{N}) = 20.44$ mb. All calculations were performed by using the GAUSSIAN98 [17] package of programs, and the results are summarized in Table 1.

$$C_Q(\mathrm{MHz}) = e^2 Q q_{zz} h^{-1}, \quad (1)$$

$$\eta_Q = \left|\left(q_{xx} - q_{yy}\right)/q_{zz}\right|, \left(0 < \eta_Q < 1\right). \quad (2)$$

## References


1. Iijima S (1991) Nature 354:56
2. Iijima S, Ichihashi T, Ando Y (1992) Nature 356:776
3. Ge M, Sattler K (1994) Appl Phys Lett 64:710
4. Ge M, Sattler K (1994) Chem Phys Lett 220:192
5. Qu CQ, Qiao L, Wang C, Yu SS, Zheng WT, Fu YZ, Jiang Q (2008) Solid State Commun 146:399
6. Zhang HZ, Zhao Q, Yu J, Yu DP, Chen Y (2007) J Phys D Appl Phys 40:144
7. Azevedo S, De Brito F, Mota R (2006) Int J Quant Chem 106:1907
8. Machado M, Piquini P, Mota R (2004) Chem Phys Lett 392:428
9. Rubio A, Corkill JL, Cohen ML (1994) Phys Rev B 49:5081
10. Bourgeois L, Bando Y, Han WQ, Sato T (2000) Phys Rev B 61:7686
11. Terauchi M, Tanaka M, Suzuki K, Ogino A, Kimura K (2000) Chem Phys Lett 324:359
12. Loiseau A, Willaime F, Demoncy N, Hug G, Pascard H (1996) Phys Rev Lett 76:4737
13. Das TP, Han EL (1958) Nuclear quadrupole resonance spectroscopy. Academic, New York
14. Mirzaei M, Hadipour NL, Seif A, Giahi M (2008) Physica E 40:3060
15. Giahi M, Mirzaei M (2009) Z Naturforsch A 64:251
16. Pyykkö P (2001) Mol Phys 99:1617
17. Frisch MJ, Trucks GW, Schlegel HB, Scuseria GE, Robb MA, Cheeseman JR, Zakrzewski VG, Montgomery JA Jr, Stratmann RE, Burant JC, Dapprich S, Millam JM, Daniels AD, Kudin KN, Strain MC, Farkas O, Tomasi J, Barone V, Cossi M, Cammi R, Mennucci B, Pomelli C, Adamo C, Clifford S, Ochterski J, Petersson GA, Ayala PY, Cui Q, Morokuma K, Malick DK, Rabuck AD, Raghavachari K, Foresman JB, Cioslowski J, Ortiz JV, Baboul AG, Stefanov BB, Liu G, Liashenko A, Piskorz P, Komaromi I, Gomperts R, Martin RL, Fox DJ, Keith T, Al-Laham MA, Peng CY, Nanayakkara A, Gonzalez C, Challacombe M, Gill PMW, Johnson B, Chen W, Wong MW, Andres JL, Gonzalez C, Head-Gordon M, Replogle ES, Pople JA (1998) GAUSSIAN 98. Gaussian Inc., Pittsburgh